Bond Graph Modeling of Planar Prismatic Joints

T.K. Bera*, A.K. Samantaray, and R. Karmakar
Department of Mechanical Engineering, Indian Institute of Technology, Kharagpur, India

* Corresponding author (email: tarunkumarbera@gmail.com)

Abstract

A planar mechanism is considered to be composed of a set of rigid bodies, which are constrained together through a set of joints. This paper discusses bond graph modeling of planar prismatic or slider joints. The developed bond graph model generates a well-computable simulation model and accurately calculates the dynamic loads. The model is validated through numerical simulations performed on an example mechanism.

Keywords: Bond graph, Multibody systems, Mechanisms.

1 Introduction

Two types of joints are generally used in robots: revolute joint and prismatic joint. The prismatic joint constitutes purely linear motion (single degree of freedom) along its axis. In prismatic joint, the direction of joint axis defines the direction of relative translation between two links. This motion is very much common in hydraulic and pneumatic cylinder. The prismatic joints are also used in connecting different links of robot mechanisms, axially moving beams and spacecrafts [1]. Multi-body systems consist of rigid and elastic bodies, joint components, passive coupling elements, and active coupling elements. The four basic joint components are translational joint, revolute joint, double translational joint, and double translational-revolute joint [2]. The slider contact forces change for different values of the slider inertia. At low speeds, the effect of the slider inertia may be neglected but at relatively high speeds, it must be included [3]. In this paper, we emphasize on development of bond graph models of prismatic members with proper mass distribution. We develop the bond graph model of a slider element with proper representation of contact forces. Although simple kinematic relations are used to construct this bond graph model, the model by itself takes care of coriolis and centrifugal forces due to the inherent power conservative properties of a true bond graph. This model shows the power and the modularity of bond graph modelling in dealing with complex mechanisms. The simulation results from this model are compared with the analytical results.

2 Modeling of Prismatic member

A schematic view of a planar piston-cylinder model, which is a prismatic member, is shown in Fig. (1). The main advantage of bond graph model is that the radial (centripetal force and others) and tangential forces (Coriolis force and others) acting at different points of the model need not be calculated. Only kinematic relations between velocities are required for model construction and the power conservative junction structure in the bond graph model yields proper equations of motion. Simulations supported by theoretical bond graph model of the actual system determine these dynamic forces. On the contrary, all forces must be explicitly derived beforehand for a Simulink model. Moreover, the bond graph model offers possibilities to include connections to other members as well as to couple the model to the models of the hydraulic system and its controllers.

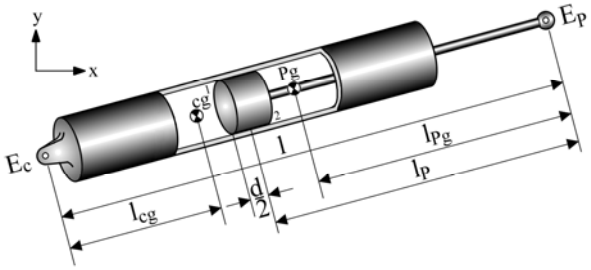

Fig. 1: Schematic of a piston-cylinder model.

The velocities of the end points E_c (x_1, y_1) and E_P (x_2, y_2) of the planar piston-cylinder model are expressed in terms of the linear velocities and of the center of gravity of the cylinder and piston-rod assembly, respectively, in the x–y plane and the rotational velocities of the same about the z–axis as follows:

$$\dot{x}_1 = \dot{x}_{cg} + l_{cg}\dot{\theta}_{cg}\sin\theta_{cg}, \quad (1)$$

$$\dot{y}_1 = \dot{y}_{cg} - l_{cg}\dot{\theta}_{cg}\cos\theta_{cg}, \quad (2)$$

$$\dot{x}_2 = \dot{x}_{Pg} - l_{Pg}\dot{\theta}_{Pg}\sin\theta_{Pg}, \quad (3)$$

$$\dot{y}_2 = \dot{y}_{Pg} + l_{Pg}\dot{\theta}_{Pg}\cos\theta_{Pg}. \quad (4)$$

The nomenclatures of different variables used in the model are given in the Appendix.

Differentiating contemporary length (l) between two points E_c and E_P with respect to time, one obtains

$$\dot{l}=\left(\frac{x_1-x_2}{l}\right)(\dot{x}_1-\dot{x}_2)+\left(\frac{y_1-y_2}{l}\right)(\dot{y}_1-\dot{y}_2) \quad (5)$$

Normal velocities at the contact point 1 on the cylinder and on the piston are

$$V_{c_1}=-\sin\theta_{cg}\dot{x}_{cg}+\cos\theta_{cg}\dot{y}_{cg}+\left(l-l_P-l_{cg}-d/2\right)\dot{\theta}_{cg} \quad (6)$$

and

$$V_{P_1}=-\sin\theta_{Pg}\dot{x}_{Pg}+\cos\theta_{Pg}\dot{y}_{Pg}-\left(l_P-l_{Pg}+d/2\right)\dot{\theta}_{Pg} \quad (7)$$

Normal velocities at the contact point 2 on the cylinder and on the piston are

$$V_{c_2}=-\sin\theta_{cg}\dot{x}_{cg}+\cos\theta_{cg}\dot{y}_{cg}+\left(l-l_P-l_{cg}+d/2\right)\dot{\theta}_{cg} \quad (8)$$

$$V_{P_2}=-\sin\theta_{Pg}\dot{x}_{Pg}+\cos\theta_{Pg}\dot{y}_{Pg}-\left(l_P-l_{Pg}-d/2\right)\dot{\theta}_{Pg} \quad (9)$$

3 Bond Graph Modeling of Prismatic Member

Equations (1–9) are sufficient to construct the augmented bond graph model of the piston-cylinder system under consideration as shown in Fig. (2).

The different multipliers in Eqs. (1–9) are used as transformer moduli of MTF elements in the model. They are $\mu_1=l_{cg}\sin\theta_{cg}$, $\mu_2=-l_{cg}\cos\theta_{cg}$, $\mu_3=-1/\sin\theta_{cg}$, $\mu_4=1/\cos\theta_{cg}$, $\mu_5=1/\left(l-l_P-l_{cg}-d/2\right)$, $\mu_6=1/\left(l-l_P-l_{cg}+d/2\right)$, $\mu_7=(x_1-x_2)/l$, $\mu_8=(y_1-y_2)/l$, $\mu_9=-l_{Pg}\sin\theta_{Pg}$, $\mu_{10}=l_{Pg}\cos\theta_{Pg}$, $\mu_{11}=-\sin\theta_{Pg}$, $\mu_{12}=\cos\theta_{Pg}$, $\mu_{13}=-\left(l_P-l_{Pg}+d/2\right)$ and $\mu_{14}=-\left(l_P-l_{Pg}-d/2\right)$.

The masses (M_P,M_c) and the moment of inertias (J_P,J_c) of the piston and cylinder, respectively, are modelled by the I-elements connected to the 1-junctions representing the velocities of the centre of gravity of the two in the inertial frame. The modulated transformers with moduli μ_7 and μ_8 are used to calculate the relative velocity between the piston and the cylinder at a 0-junction and the friction between the piston and the cylinder is modelled by an R-element (r_f) at that junction. The sources of efforts at the 1-junction indicate the joint forces. The normal velocity at the contact point on the cylinder is made equal to normal velocity at the contact point on the piston by providing higher values of contact stiffness and damping parameters.

4 Case Study: Rapson Slide

Rapson slide is considered here as an example application. This mechanism is commonly fitted to steer gear system of ships. It works with higher hydraulic pressure. It is used to control the rudder of large ships. Here, the slider replaces piston and rod replaces cylinder of piston-cylinder model. The tiller E_cE_P is keyed to the point E_c. The tiller makes an angle θ_{Pg} with the horizontal. The block slides on the rod. The contemporary length between the hinge E_c and the slider is l. The distance between the hinge E_c and the centre of gravity of the rod is l_{cg}. Only horizontal force acts at the centre of the slider as shown in Fig. (3) so that slider slides along the rod with velocity V and the rod rotates with an angular velocity ω about the hinge E_c.

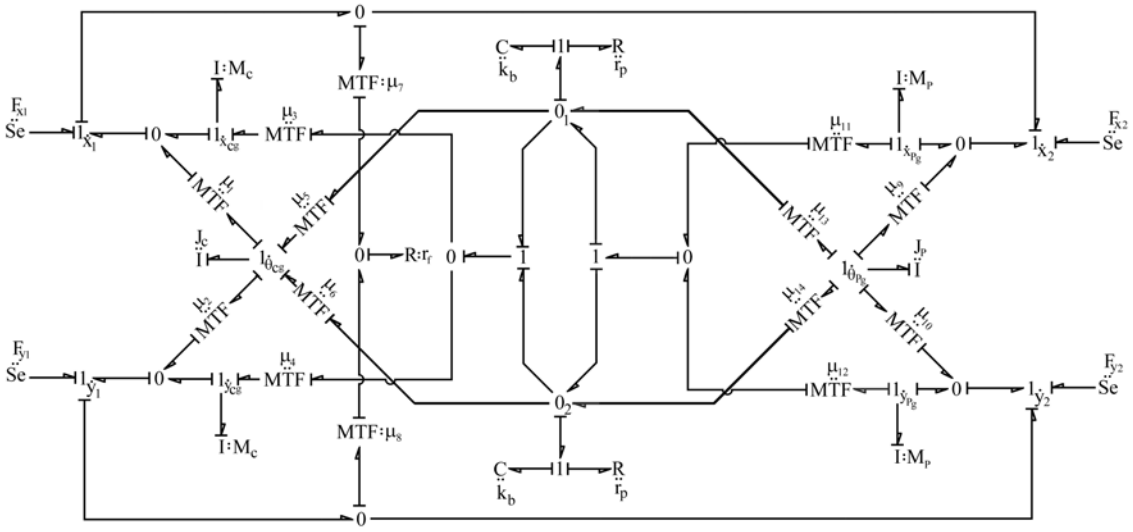

Fig. 2: Bond graph model of piston-cylinder.

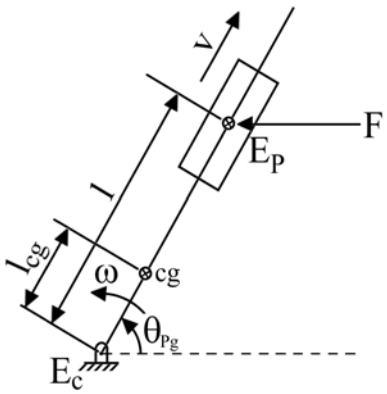

Fig. 3: Schematic of Rapson slide.

The distances l_{Pg} and l_P (Fig. (1)) are set to zero. With these boundary conditions, the piston-cylinder model is equivalent to Rapson slide model. Its bond graph model is developed in the next section.

5 Bond Graph Modeling of Rapson Slide

The bond graph model of Rapson slide which is shown in Fig. (4), is obtained by slightly modifying the bond graph model of piston-cylinder. The inertia elements of the slider and rod are modeled by the I-elements connected to the 1-junctions. As the end point of the rod E_c is fixed, there is no motion there, which is imposed by putting zero flow sources. A coupling capacitor [4] or pad [5–7] can be added to the system at appropriate locations for avoiding the differential causalities. The normal velocity at the contact point on the rod is made equal to normal velocity at the contact point on the slider by providing higher values to contact stiffness and damping parameters.

6 Simulink Modeling of Rapson Slide

The forces acting in the radial direction, including the centrifugal force, at the point E_P is

$$M_P\left(\ddot{l} - \dot{\theta}_{Pg}^2 l\right) + F\cos\theta_{Pg} = 0\,. \qquad (10)$$

The moment acting in the tangential direction, including Coriolis force, at the point E_P is

$$J_{eqv}\ddot{\theta}_{Pg} + 2M_P\dot{\theta}_{Pg}l\dot{l} - Fl\sin\theta_{Pg} = 0\,, \qquad (11)$$

where, the total equivalent moment of inertia at point E_c is

$$J_{eqv} = M_P l^2 + J_P + M_c l_{cg}^2 + J_c \qquad (12)$$

A Simulink block diagram model (not given) can be constructed by using Eqs. (10–12). The results of simulation from the Simulink model are compared with those from the bond graph model as shown in Fig. (5).

7 Simulation Results and Validation of the Model

The parameter values used in the simulation are chosen properly. The distance between the centre of gravity of the piston and the end point of the piston rod E_P and as well as the distance between the centre of gravity of the piston-rod assembly and the end point of the piston rod E_P are set to zero. Initially the Rapson slide makes an angle of 36.87° with the horizontal. The distance between the points E_c and the centre of gravity of the piston is 5 m. A horizontal force of constant magnitude 1 N acts at the centre of gravity of the slider. The parameter values and the initial conditions used in the simulation are given in Tables 1 and 2, respectively.

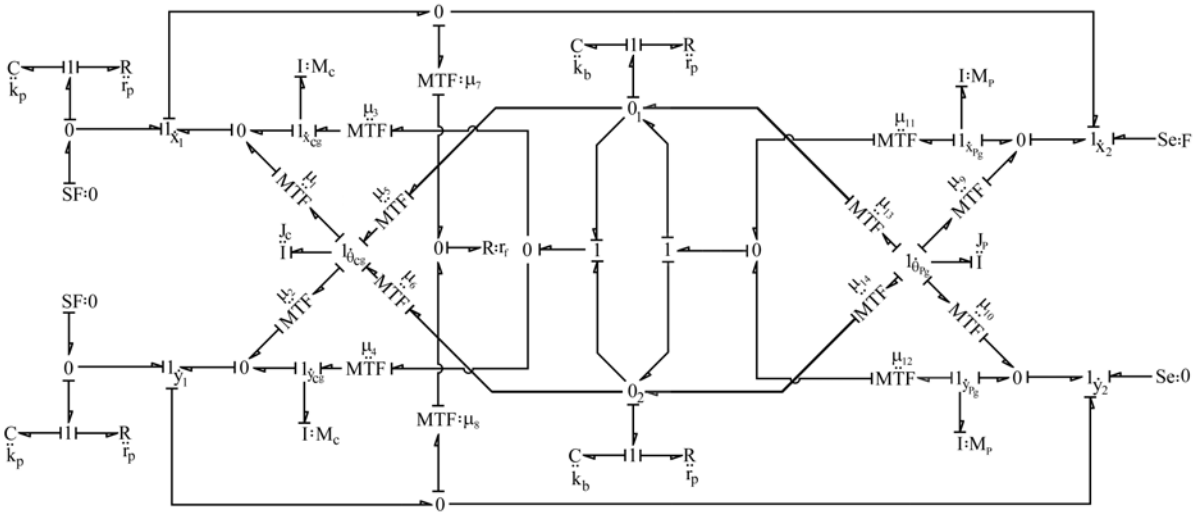

Fig. 4: Bond graph of Rapson Slide.

Table-1: Parameter values

Parameter Values		
d =0.4 m	l =5 m	l_{cg} =1.5 m
l_p =0.0 m	l_{pg} =0.0 m	k_b =10^5 N/m
k_p =10^5 N/m	r_p =10^3 N.s/m	F =1 N
J_c =1 kg.m^2	J_p =1 kg.m^2	M_c =1 kg
M_p =1 kg	r_f =0.0 N.s/m	

Table-2: Initial conditions

Initial Values		
x_c =1.2 m	y_c =0.9 m	x_p =4 m
y_p =3 m	x_1 =0 m	y_1 =0 m
θ_c =0.6435011 rad	θ_p =0.6435011 rad	

The bond graph model and the Simulink model are simulated. The angular displacement, angular velocity and the angular acceleration of the slider are plotted in Fig. (5). The marginal errors (though not visible by naked eye) between this two models may be attributed to the extra dynamics (contact forces and pads) modelled in the bond graph model. The results validate the bond graph model of the Rapson slide. The normal forces at the two contact points 1 and 2 between the cylinder and piston are shown in Fig. (6). It also depicts the frictional forces between the piston and slider when the coefficient of kinematic friction

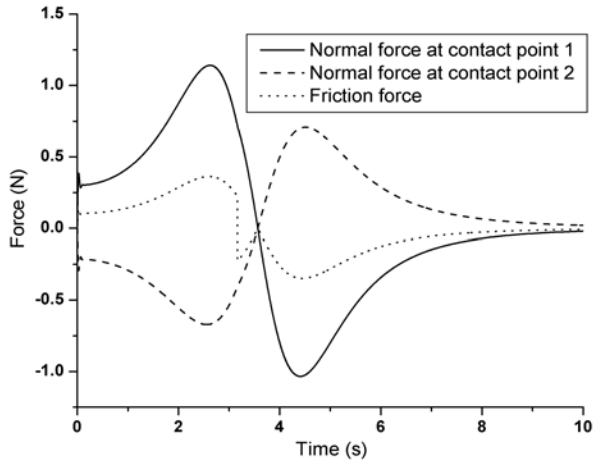

Fig. 6: Normal forces at the contact points 1 and 2, and (b) Frictional force between the piston and cylinder.

$\mu_k = 0.2$. The constitutive relation for the non-linear R-element (r_f) representing friction between the cylinder (slider) and the piston is given by

$$e_f = \mu_k \left(|e_{N1}| + |e_{N2}| \right) \text{sign}\left(f_f \right), \qquad (13)$$

where e_{N1} and e_{N2} are the normal contact forces between the piston and the cylinder and e_f and f_f are respectively the effort and flow variables.

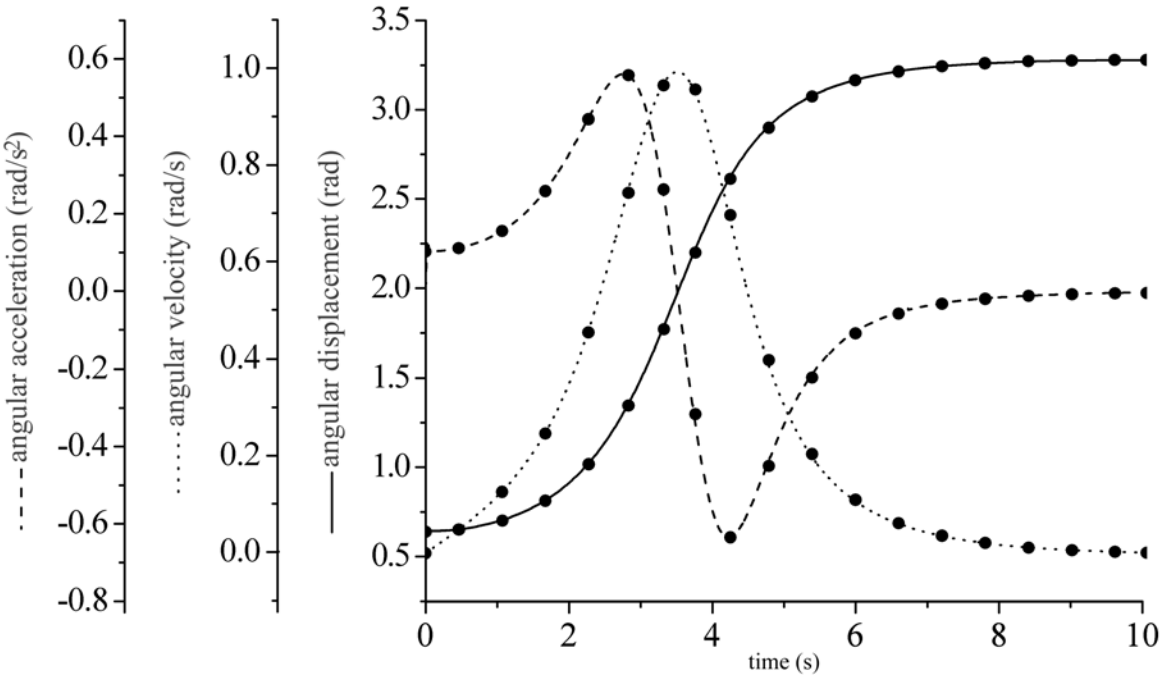

Fig. 5: Angular displacement, velocity and acceleration for the centre of the slider. (a) Line indicates Bond graph model, and (b) Scatter points indicate Simulink model.

8 Conclusion

A bond graph model of a planar slider component with two moving contact points was developed from the first principles. The corresponding dynamics obtained from simulation results were compared with results obtained from another approach to validate the developed model. Though the bond graph of the slider (Fig. (4)) is drawn from kinematic relations, the power conservative nature of the bond graph junction structure also ensures that the constraints between the forces and moments are simultaneously satisfied. This allows for the calculation of the reaction forces at the joints, contact forces and frictional forces. The bond graph model is modular and it can be easily interfaced with other models and can be extended by adding other dynamical parts, such as addition of oil hydraulics and solenoid-based spool valve control system. The equations of motion are derived from the bond graph model through well-established algorithmic ways. This modularity establishes bond graph as an efficient hierarchical object oriented modelling tool. As a final note, a bond graph model can be used for calculation of the inverse dynamics by using an inverse model with appropriate causalities. The inverse model is useful to develop control systems for systems employing the manipulator of the kind discussed here, e.g., vehicle suspension systems, planar Stewart platforms, forklifts, excavators, etc., where inverse dynamics is required for actuator sizing and robust control.

References

[1] J. Yuh, T. Young, Y.S. Baek, "Modeling of a flexible link having a prismatic joint in robot mechanism–experimental verification," *IEEE*, CH2750-8/89/0000/0722, 1989, pp. 722-727.

[2] W. Marquis-favre, E. Bideaux, S. Scavarda, "A planar mechanical library in the AMESim simulation software. Part II: Library composition and illustrative example," *Simulation Modelling Practice and Theory*, Vol. 14, 2006, pp. 95–111.

[3] E.D. Stoenescu, D.B. Marghitu, "Effect of prismatic joint inertia on dynamics of kinematic chains," *Mechanism and Machine Theory*, Vol. 39, 2004, pp. 431–443.

[4] A. K. Samantaray, B. Ould Bouamama, *Model-based Process Supervision*, Springer Verlag, London, 2008.

[5] A. Mukherjee, R. Karmakar, and A. K. Samantaray, *Bond Graph in Modeling, Simulation and fault Identification*, CRC Press, FL, 2006.

[6] A. K. Ghosh, A. Mukherjee, M. A. Faruqi, "Computation of driving efforts for mechanisms and robots using bond graphs," *Journal of Dynamic Systems, Measurement and Control, Transactions of ASME*, Vol. 113(4), 1991, pp. 744–748.

[7] P. M. Pathak, R. P. Kumar, A. Mukherjee, A. Dasgupta, "A scheme for robust trajectory control of space robots," *Simulation Modelling Practice and Theory*, Vol. 16, 2008, pp. 1337–1349.

Appendix

Table-3: Nomenclature

E	End point
F	Force
J	Polar moment of inertia
K_i	Stiffness
M	Mass
V	Normal velocity
d	Width of the piston
e_i	Effort in the i^{th} bond
f_i	Flow in the i^{th} bond
g	Acceleration due to gravity
k_p	Stiffness of pad
l	Distance between E_c and E_P
l_{cg}	Distance between point E_c and centre of gravity of cylinder
l_p	Distance between point E_P and center of gravity of piston
l_{Pg}	Distance between point E_P and centre of gravity of piston-rod
r	Damping
r_p	Damping of pad
t	Time
x	Displacement in x-direction
y	Displacement in y-direction
$\dot{x}$	Velocity in x-direction
$\dot{y}$	Velocity in y-direction
θ	Rotation about z-axis
$\dot{\theta}$	Angular velocity about z-axis
μ	Transformer modulus
Subscripts	
P	Piston/Slider
Pg	Center of gravity of slider
b	Contact
c	Cylinder/Rod
cg	Center of gravity of cylinder
f	Friction
1,2	Contact point number